

Optical properties of A_2CuCl_4 layer perovskites under pressure. Structural correlations

F. RODRÍGUEZ¹, M. HANFLAND², J.P. ITIÉ³ AND A. POLIAN³

¹ DCITIMAC, Facultad de Ciencias, University of Cantabria, 39005 Santander, Spain

² ESRF, BP220, 156 rue des Martires, 38043 Grenoble Cedex, France

³ LURE, Centre Universitaire Paris-Sud, 91898 Orsay Cedex, France

Abstract: This work investigates the optical spectra of Cu(II) layered perovskites under pressure. The aim is to establish correlations between the metal-to-ligand charge transfer spectra and the local structure around the Cu(II). For this purpose, X-ray diffraction (XRD) and X-ray absorption (XAS) experiments on the title compounds were performed as a function of pressure in the 0-100 kbar range. The pressure redshift experienced by the first charge transfer band correlates with a reduction of the Jahn-Teller (JT) distortion of the hexachloride Cu(II) complex. Interestingly, the application of pressure to these layer compounds induces octahedron tilts rather than a reduction of the in-plane antiferrodistortive structure related to the cooperative JT structure. This reflects the stiffness of the JT Cu complex whose local bulk modulus is an order of magnitude greater than the crystal bulk modulus.

Key words: Pressure spectroscopy, XAS, XRD, Jahn-Teller systems, Cu(II)-layered perovskites

1. INTRODUCTION

The A_2CuCl_4 ($A=C_nH_{2n+1}NH_3$; $n=1-3$) layered compounds present a large variety of interesting physical phenomena associated with antiferrodistortive structure displayed by the Jahn-Teller (JT) axially elongated $CuCl_6^{4-}$ complexes [1-6]. They have attracted interest as two-dimensional ferromagnets with $T_c=10$ K [1], as related material to high T_c superconductors,

as an organic/inorganic hybrid layered system, and as piezochromic materials [2]. In the last years there has been an intense activity to investigate the behavior of these materials under hydrostatic pressure, in particular, for exploring pressure-induced structural transitions associated with the disappearance of the antiferrodistortive structure [3-6]. This phenomenon is noteworthy since it must lead to a switch in the magnetic behavior from ferromagnetic at zero pressure to antiferromagnetic at high pressure.

The optical spectra of layered systems A_2CuCl_4 are mainly governed by electronic transitions associated with the Crystal Field (CF) levels of the d^9 configuration of Cu^{2+} , and the $Cl^- \rightarrow Cu^{2+}$ Charge Transfer (CT) states, related to the crystal band gap. To a great extent, these properties can be understood on the basis of the $CuCl_6^{4-}$ complex unit, thus the study of the optical properties of isolated $CuCl_6^{4-}$ is important to achieve this goal. In particular, we are interested in structural correlations between optical CF and CT spectra and the complex geometry: symmetry and Cl-Cu bond distances. However this task is difficult to accomplish on dealing with Cu^{2+} -doped A_2MCl_4 ($M = Cd, Mn$; $A = C_nH_{2n+1}NH_3$; $n=1-3$) since, at variance with pure A_2CuCl_4 materials, neither X-Ray Diffraction (XRD), nor X-ray Absorption Spectroscopy (XAS) can be efficiently employed in diluted impurity systems to establish such correlations.

In general, the optical properties of JT $CuCl_6^{4-}$ and CuF_6^{4-} complexes strongly depend on the local structure around Cu^{2+} . The occurrence of a given coordination geometry is mainly determined by the linear electron-vibration coupling between the octahedral $e_g(x^2-y^2, z^2)$ d-orbitals and vibrational modes of $e_g(Q_7, Q_6)$ symmetry: $E \otimes e$ JT effect. Second order JT coupling, anharmonicity and crystal anisotropy determine the final coordination geometry of the complex [7,8]. Thus a great variety of structures can be found in Cu^{2+} -doped materials depending on the crystallographic structure of the host crystal. For $CuCl_6^{4-}$ and CuF_6^{4-} complexes, the coordination geometry can vary from the elongated tetragonal to the compressed one (D_{4h}), through different orthorhombic intermediates (D_{2h}) [8]. The *elongated* fluoride CuF_6^{4-} complexes (D_{4h}) found in CuF_2 and $NaCuF_4$ [9] and the *compressed* ones (D_{4h}) found in $KCuAlF_6$ [10], $Ba_2ZnF_6: Cu^{2+}$ [11] and $K_2ZnF_4: Cu^{2+}$ [12,13] are examples of this distinct behavior. However, the situation is completely different for $CuCl_6^{4-}$. Most investigated systems exhibit axially elongated octahedra of nearly D_{4h} symmetry, even in cases, as Cu^{2+} -doped A_2CdCl_4 , where Cu^{2+} is introduced in strongly D_{4h} compressed sites [14]. Layered perovskites are very attractive systems for this purpose since they provide strongly compressed sites, $CdCl_6^{4-}$, with Cd-Cl distances of $R_{eq}=2.667 \text{ \AA}$ (4) and $R_{ax}=2.535 \text{ \AA}$ (2) for $(C_3H_7NH_3)_2CdCl_4$ [15] (Fig. 1). However, the replacement of Cu^{2+} for Cd^{2+} leads to the formation of axially *elongated* $CuCl_6^{4-}$ units, with the longest in-layer axial Cu-Cl bonds randomly distributed along either **a+b** or **a-b** crystallographic directions [16] (Fig. 1). Interestingly, this impurity configuration resembles the

antiferrodistortive structure displayed by the pure $(C_3H_7NH_3)_2CuCl_4$ in which the in-plane equatorial Cl ligand of one Cu acts as axial ligand of the nearest Cu.

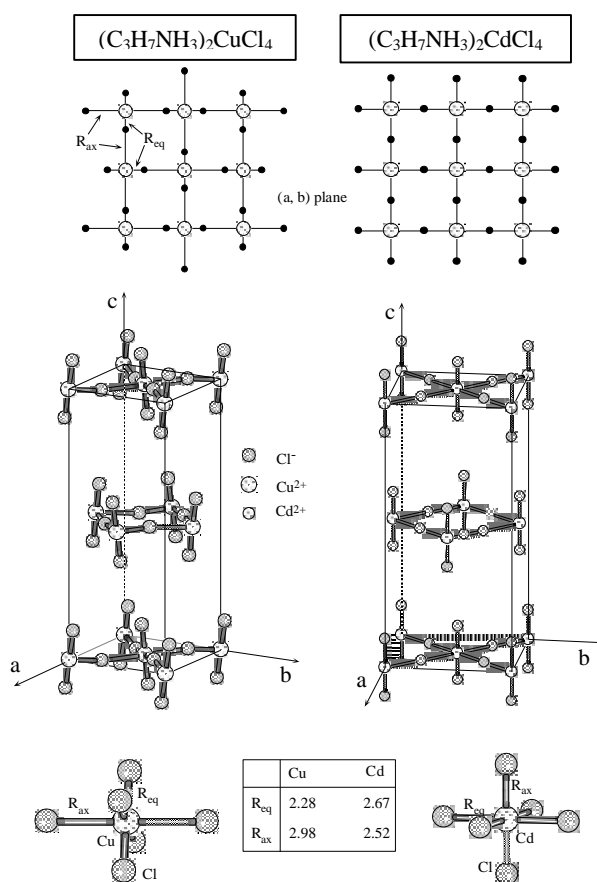


Figure 1. Schematic view of $(C_3H_7NH_3)_2CuCl_4$ and $(C_3H_7NH_3)_2CdCl_4$ perovskite layers. The alternating $CuCl_4^{2-}$ units form an antiferrodistortive structure associated with orthogonal orientations of alternating Cu-Cl bonds in the (001) plane. This structure yields a real $CuCl_6^{4-}$ coordination geometry of nearly D_{4h} symmetry, where the in-plane equatorial Cl ligand of one Cu acts as axial ligand of the nearest Cu. Note that A_2CdCl_4 provides compressed tetragonal geometry at the Cd site. The two equatorial Cl ions along *c* are terminal ligands. The orthorhombic *a*, *b* and *c* cell vectors are indicated.

This paper investigates the variation of the optical absorption spectra of A_2CuCl_4 with pressure as a function of the local structure around Cu^{2+} . The aim is twofold. Firstly, pure materials are ideal systems to establish structural correlations between pressure-induced band shifts and the corresponding changes of local structure around Cu^{2+} , using optical absorption spectroscopy, and XRD and XAS techniques, respectively. Secondly, there is an increasing interest to elucidate whether the in-plane antiferrodistortive structure in the A_2CuCl_4 crystal series, or the associated JT distortion of $CuCl_6^{4-}$, can be released under pressure. Furthermore, the color of these crystals, which is basically determined by the optical window formed by the first $e_g(\pi) \rightarrow b_{1g}(x^2-y^2)$ CT band placed at 26000 cm^{-1} , and the CF band of highest energy located around 12000-17000 cm^{-1} , strongly depends on the $CuCl_6^{4-}$ coordination geometry [6]. Therefore structural changes of the complex geometry induced by pressure may lead to interesting piezochromic effects. Moreover, these changes will probably involve structural transformations of the JT complex from an in-plane axially elongated $CuCl_6^{4-}$ to either an octahedral O_h or a compressed tetragonal D_{4h} geometry, provided that axial Cl ligands lie on the layer. In either case an important redshift of the CT band and the CF bands should be expected.

Pressure-induced CT redshifts have been observed in both pure A_2CuCl_4 [4,6,17] and Cu^{2+} -doped A_2CdCl_4 [18]. In all cases, the first CT band shifts about 2000 cm^{-1} from ambient pressure to 100 kbar. This has been explained in terms of changes of local structure around Cu^{2+} according to expectations for CT shifts from electronic structure calculations [19]. CT redshifts induced by pressure in $CuCl_6^{4-}$ are possible whatever the equatorial distance, R_{eq} , increases upon pressure. From the crystal structure of Fig. 1, an increase of R_{eq} upon pressure is possible if the in-plane Cl ligands move in the middle of the Cu-Cu ions.

Evidence of this structural variation was first given in [4] for $(C_2H_5NH_3)_2CuCl_4$ and in [14,18] for Cu^{2+} -doped A_2CdCl_4 using optical spectroscopy techniques. The pressure dependence of the Raman spectra and the variation of the $Cl^- \rightarrow Cu^{2+}$ CT spectra in A_2CuCl_4 were explained on the assumption of a progressive reduction of the $CuCl_6^{4-}$ axial distortion with pressure [4-6,17,18]. However no correlation has been established between the variation of the optical spectra of A_2CuCl_4 and the corresponding structural changes undergone upon pressure.

In this work we present XAS and XRD measurements under pressure in $(C_3H_7NH_3)_2CuCl_4$ in the 0-100 kbar range. The results are compared with previous findings on the optical properties of the same material. A salient conclusion of this work is that a CT redshift in pure systems is compatible with an anisotropic reduction of the Cu-Cl distances. A perturbed octahedron model for explaining the observed pressure redshifts has been reported elsewhere [6]. The main idea of the model is to balance two opposite contributions involved in the CT shift: i) the blueshift induced by a decrease of the average Cu-Cl distance

(complex volume) and, ii) the redshift related to the reduction of axial distortion upon pressure. The competition between these two processes determines the sign of the pressure shift.

With these experiments, we also expect to elucidate whether the effect of hydrostatic pressure on these compounds is to reduce the longest in-plane Cu-Cl distance yielding to a reduction of the Jahn-Teller distortion or it induces tilts of the $CuCl_6^{4-}$ octahedra. Each process should lead to different compound properties.

2. EXPERIMENTAL

Single crystals of A_2CuCl_4 and Cu^{2+} -doped A_2CdCl_4 examined in pressure experiments, were grown from solution as described elsewhere [16,17]. The optical absorption experiments under pressure were reported in Refs [4-6,14,17,18].

X-ray diffraction (XRD) under pressure was performed in the ID9 white beam station at the European Synchrotron Radiation Facility (ESRF) in Grenoble. Experiments were done on a diamond anvil cell (DAC) at room temperature using nitrogen as pressure transmitter. X-ray powder diffractograms were obtained as a function of pressure in the 0-110 kbar range using wavelength, $\lambda = 0.4124 \text{ \AA}$, which is far enough from the spectral region of the diamond absorption.

XAS experiments under pressure have been performed at the absorption setup XAS10 of the D11 beamline at LURE (Orsay). The EXAFS spectra of the investigated $(C_3H_7NH_3)_2CuCl_4$ layer perovskite were measured at the Cu K-edge ($E_0 = 8.977 \text{ keV}$) at room temperature using dispersive EXAFS in the 8.9-9.3 keV range. This experimental setup has been proved to be very sensitive for obtaining suitable EXAFS oscillations in a wavelength range where the diamond anvil absorption is very strong. LURE provides adequate beam coherence and intensity to do EXAFS under pressure. XAS experiments under pressure at the even more absorbing Fe K-edge confirms the D11 capability [20]. The pressure was applied with a membrane-type DAC employing paraffin oil as pressure transmitter. EXAFS spectra have been analysed on the basis of a $CuCl_6^{4-}$ unit with three different Cu-Cl distances: R_{eq1} , R_{eq2} and R_{ax} .

The pressure was measured through the R-line shift of Ruby chips introduced in the hydrostatic cavity.

3. RESULTS AND DISCUSSION

Figure 2 and 3 show the variation of the EXAFS spectra and the XRD

powder diagrams, respectively, as a function of pressure. At ambient pressure EXAFS data mainly reflect the fourfold coordination geometry associated with the short Cu-Cl bonds, and also the twofold coordination related to the axial ligands. The local distances at $P = 2$ kbar derived from Fig. 1, $R_{\text{eq}} = 2.29 \text{ \AA}$ and $R_{\text{ax}} = 2.94 \text{ \AA}$ are close to the bond distances derived from X-ray diffraction ($R_{\text{eq}} = 2.29 \text{ \AA}$ and $R_{\text{ax}} = 3.04 \text{ \AA}$).

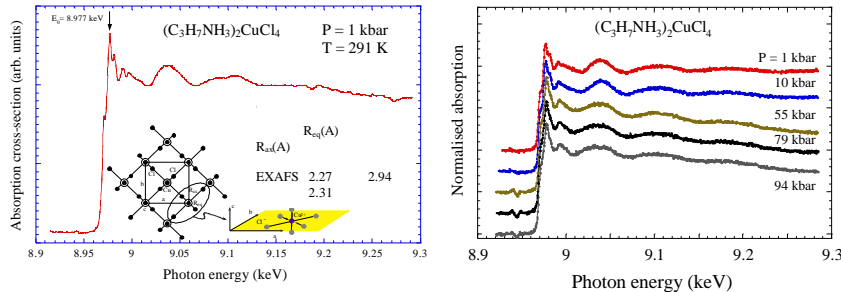


Figure 2. EXAFS of $(\text{C}_3\text{H}_7\text{NH}_3)_2\text{CuCl}_4$ powders at room temperature as a function of pressure. The calculated spectrum has been obtained by fitting using the values of $R_{\text{eq}1}$, $R_{\text{eq}2}$ and R_{ax} represented in Fig. 4.

A puzzling feature of Fig. 2 is the slight variation of the EXAFS oscillations upon pressure in the 0-100 kbar range. Nevertheless, it contrasts with the corresponding variation undergone by the Bragg peaks in XRD experiments (Fig. 3), thus suggesting a different pressure behavior of the local structure around Cu^{2+} and the crystal cell (lattice parameters). The crystal compressibility seems to be much higher than the local compressibility associated with CuCl_6^{4-} . The stiffness of the intra Cu-Cl bonds of CuCl_6^{4-} reflects the molecular character of the $(\text{C}_3\text{H}_7\text{NH}_3)_2\text{CuCl}_4$ layered structure.

The variations of local distances and lattice parameters under pressure derived from EXAFS and XRD are shown in Fig. 4. The XRD diagrams can be accounted for on the basis of the ambient structure (Orthorhombic $Pbca$) [21] in the explored pressure range. The cell volume and the lattice parameters vary continuously with pressure and no evidence of pressure-induced phase transition has been detected (Fig. 4). The volume $V(P)$ can be properly described through a Murnaghan equation of state with $B_0 = 67$ kbar and $B' = 7$. It is worth noting the different compressibility of the crystal within the (001) layer and perpendicular to it; the bulk modulus derived from pressure variations of $R_{\text{Cu-Cu}} = 1/2(a^2 + b^2)^{1/2}$ and c , are $B_{\text{Cu-Cu}} = 85$ kbar and $B_c = 60$ kbar, indicating that the crystal is more compressible along c than in-plane, according to its layered structure (Fig. 4). However, the variation of the in-plane axial and equatorial Cu-Cl distances is

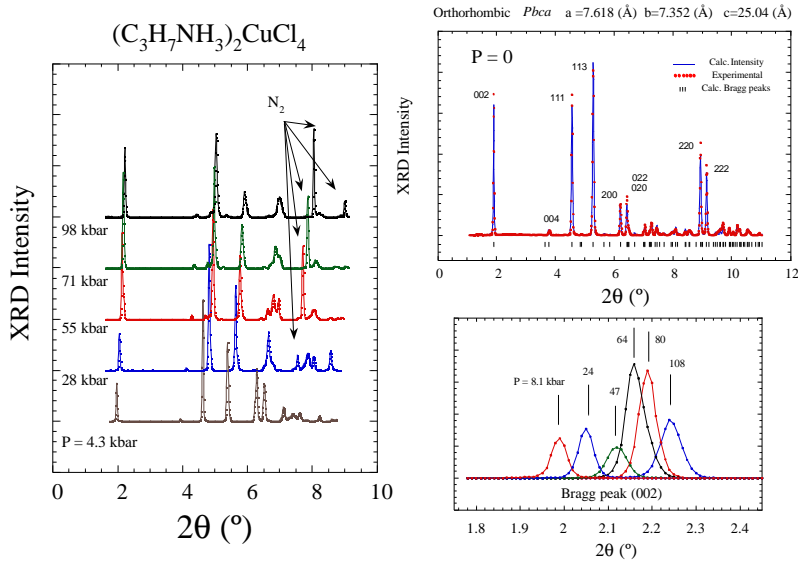


Figure 3. Variation of the XRD diagrams of $(C_3H_7NH_3)_2CuCl_4$ with pressure at room temperature. Bragg peaks were indexed according to an Orthorhombic $Pbca$ space group. The simulated XRD diagram at $P = 0$ and a detailed variation of the (002) peak are given in separated plots.

rather different to that found for the R_{Cu-Cu} . Figure 5 compares the pressure-induced variations of R_{Cu-Cu} derived from XRD, and $R_{ax} + R_{eq}$ from XAS. Note that the observed variations can not be explained on the assumption that the axial lie on the (001) plane. If it occurs, the pressure dependence of $(R_{eq} + R_{ax})$ should be close to that corresponding to R_{Cu-Cu} , according to the crystal structure shown in Fig. 1:

Actually, this is not observed in Fig. 5 thus suggesting the occurrence of $CuCl_6^{4-}$ tilts under pressure. The present result is not surprising since the family of layered perovskites shows a wide variety of structural modifications related to

$$\frac{\partial(R_{eq} + R_{ax})}{\partial P} = \frac{\partial R_{Cu-Cu}}{\partial P}$$

tilts of the $CuCl_6^{4-}$ octahedra. The $AMnF_4$ (M: Na, K, Rb, Cs) series involving antiferrodistortive structures of JT Mn^{3+} ions [22,23], as well as the A_2CuCl_4 series of JT Cu^{2+} are examples of this behavior. The smaller cell volume is the more pronounced tilts of the MnF_6^{3-} and $CuCl_6^{4-}$ octahedra [22,24].

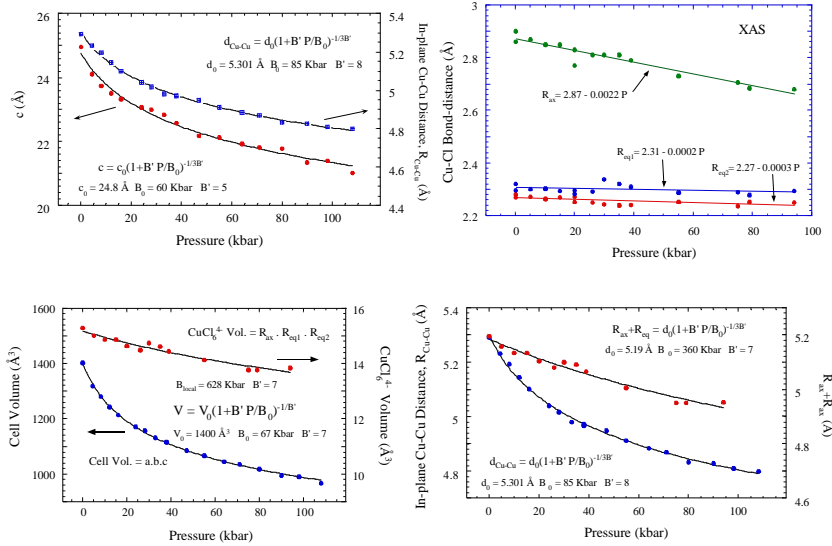


Figure 4. Above: Pressure dependence of R_{ax} , R_{eq1} , and R_{eq2} derived from XAS (Fig. 2) corresponding to the sixfold coordination local structure around the Cu, and the lattice parameter c , the Cu-Cu distance, $R_{Cu-Cu} = 1/2[a^2 + b^2]^{1/2}$, obtained from XRD corresponding to $(C_3H_7NH_3)_2CuCl_4$ at room temperature. Full lines are least square fitting of data to the Murnaghan type equation of state and linear fits for XAS. Below: Comparison between pressure variations of the crystal cell and the $CuCl_6^{4-}$ local structure. Note that the local compressibility of $CuCl_6^{4-}$ is much smaller than the $(C_3H_7NH_3)_2CuCl_4$ crystal

The behavior of the $CuCl_6^{4-}$ local structure upon pressure, shown in Figs. 4 and 5, is in agreement with this behavior. Reduction of crystal volume induces a significant decrease of the $CuCl_6^{4-}$ tetragonal distortion: $\Delta R_{ax} \approx 10 \Delta R_{eq}$. However, there is no way to correlate this variation with the proposed structural distortion for $CuCl_6^{4-}$ tending to reduce the axial distance and to increase the equatorial distance to a situation where $R_{ax} \approx R_{eq}$. The different pressure behavior of $R_{eq} + R_{ax}$, and R_{Cu-Cu} (Fig. 5) clearly indicates tilting phenomena in these compounds. The variation of the Cu-Cl-Cu tilting angle, θ , with pressure is shown in Fig. 5. Interestingly, the pressure-induced disappearance of the antiferrodistortive structure and the corresponding change of magnetic properties are not associated with a reduction of the in-plane JT distortion of $CuCl_6^{4-}$, but to rotations of the octahedra. Deviations of θ from 180° enhance the antiferromagnetic exchange interaction between Cu at expenses of the ferromagnetic interaction, greatly favored in a pure antiferrodistortive structure ($\theta = 180^\circ$). Structural correlations between the exchange interaction, $-Js_1.s_2$, and

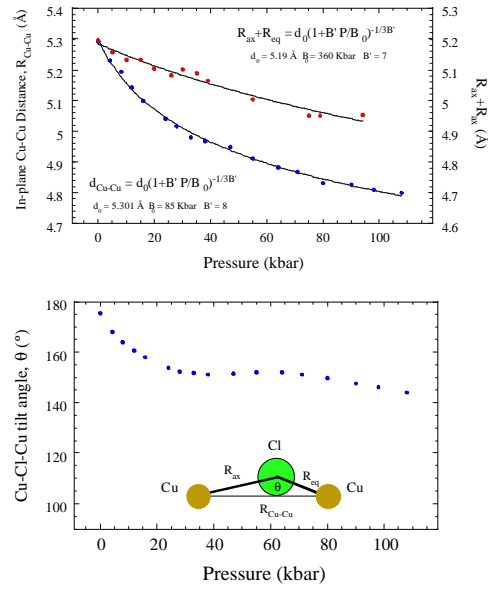


Figure 5. Above: Variation of the in-plane Cu-Cu distance, $R_{Cu-Cu} = 1/2[a^2 + tb^2]^{1/2}$ and $R_{ax} + R_{eq}$. Below: Pressure dependence of the Cu-Cl-Cu tilt angle, θ , derived from the variations of R_{Cu-Cu} and $R_{ax} + R_{eq}$

the tilt angle, $J(?)$, performed on Mn^{3+} compound series confirm this interpretation [24].

4. CONCLUSIONS AND FINAL REMARKS

The observed structural variations confirm the instability of the antiferrodistortive layered structures under pressure. Its disappearance is not related to structural changes of the $CuCl_6^{4-}$ units from an axially elongated geometry to a compressed situation as suggested previously [4,6], but to tilts of these complexes. Importantly, tilts preserve largely the axially elongated JT distortion of $CuCl_6^{4-}$ according to its strong molecular character. The JT related stiffness of the Cu-Cl bonds impedes release of the in-plane strain, favoring octahedron tilts as an effective way for accommodating axially elongated $CuCl_6^{4-}$ in a more reduced volume.

The important question arising at this point is whether the CT redshift observed in both Cu^{2+} -doped A_2CdCl_4 and pure A_2CuCl_4 materials, is just related to structural changes of $CuCl_6^{4-}$. Could a reduction of Cu-Cl distances,

$\partial R_{eq}/\partial P = -0.00015 \text{ \AA/kbar}$ and, $\partial R_{ax}/\partial P = -0.0022 \text{ \AA/kbar}$, account for the observed redshifts?

Although there is only qualitative indications of this possibility [6], it seems that the contribution of the JT distortion to the band shift plays a fundamental role in the shift process. In fact, the JT splitting associated with the CuCl_6^{4-} molecular orbitals involved in the first CT transition, the parent octahedral e_g 3d-orbitals of Cu^{2+} , $a_{1g}(z^2)$ and $b_{1g}(x^2-y^2)$, and the parent t_{1u} ($a_{1u} + e_u$) mainly p Cl ligand orbitals, contributes by more than 30% to the CT transition energy with respect to a pure octahedral complex [6]. Moreover, the JT contribution would be significantly enhanced if we consider that the main pressure effect on CuCl_6^{4-} leads to a more pronounced reduction of the JT distortion than the average bond distance ($Q_J \ll Q_{a1g}$), as is shown in Fig. 4. Similar phenomena have also been detected in the JT cooperative AMnF_4 systems [23]. An account of pressure effects on the JT distortion of MnF_6^{4-} will be reported [25].

ACKNOWLEDGMENTS

We thank Professors M. Moreno, M.T. Barriuso, J.A. Aramburu, and Doctors R. Valiente and A. Moral, for fruitful discussions and collaboration in this work. This research was supported by Caja Cantabria, and the CICYT (Project No. PB98-0190). The XAS experiments were done on the basis of the experimental proposal at the LURE in Orsay (France) under Project No 050-00.

REFERENCES

1. L.J. de Jongh and A.R. Miedema, *Advan. Phys.* **23**, 1 (1974).
2. R. Valiente and F. Rodríguez, *J. Phys. Chem. Solids*, **57**, 571 (1996)
3. , T. Sekine, T. Okuno and K. Awaga, *Chem. Phys. Lett.* **249**, 201 (1996)
4. Y. Moritomo and Y. Tokura, *J. Chem. Phys.* **101**, 1763 (1994)
5. R. Valiente, F. Rodríguez, M. Moreno and M.A. Hitchman, *Physica B* **265**, 176 (1999)
6. R. Valiente and F. Rodríguez, *Phys. Rev. B* **60**, 9423 (1999)
7. D. Reinen and M. Atanasov, *Magnetic Resonance Review* **15**, 167 (1991)
8. M.A. Hitchman, *Comments Inorg. Chem.* **15**, 197 (1994)
9. D. Oelkrug, *Structure and Bonding* **9**, 1(1971)
10. K. Finnie, L. Dubicki, E.R. Krausz and M.J. Riley, *Inorg. Chem.* **29**, 3908 (1990)
11. . D. Reinen, G. Steffen, M.A. Hitchman, H. Stratemeier, L. Dubicki, E.R. Krausz., M. Riley, H.E. Mathies., K. Recker and F. Wallrafen, *Chem. Phys*

- 155**, 117 (1991)
12. M.J. Riley, M.A. Hitchman and D. Reinen, Chem. Phys. **102**, 11 (1986)
12. M.J. Riley, L. Dubicki, G. Moran, E.R. Krausz, and I. Yamada, Chem. Phys. **145**, 363 (1990)
- 14 B.A. Moral, F. Rodríguez, R. Valiente, M. Moreno and H.U. Güdel, Z. Phys. Chem. **201**, 151 (1997)
- 15 G. Chapuis, Acta Cryst. B. **34**, 1506 (1978)
- 16 B. Baticle, F. Rodriguez, and R. Valiente, Rad. Eff. Def. Sol. **135**, 89 (1995)
- 17 R. Valiente, F. Rodriguez, M. Moreno and M.A. Hitchman, Physica B **265**, 176 (1999)
- 18 B.A. Moral and F. Rodríguez, J. Phys. Chem. Solids **58**, 1487 (1997)
- 19 M. Moreno, M.T Barriuso and J.A. Aramburu, Appl. Magn. Reson. **3**, 283 (1992)
- 20 A. Sadoc., J.P. Itié, A. Polian, S. Lefebvre, M. Bessière and Y. Calvayrac, Phil. Mag. B **70**, 855 (1994)
- 21 F. Barendregt and H. Schenk Physica, **49**, 465 (1970).
- 22 M.C. Morón, F. Palacio and S.M Clark. Phys. Rev. B, **54**, 7052 (1996)
- 23 S. Carlson and R. Norrestam Z.Kristallogr., **210**, 489 (1995)
and Private communication.
- 24 F. Palacio and M.C. Morón, *Research Frontiers in Magnetochemistry*, World Scientific. (1992)
- 25 F. Aguado, F. Rodriguez and P. Núñez, Submitted to the EHPRG'39 Meeting, Santander (2001)